CFD modeling of the flow over Pedrógão dam spillway and roller bucket

Timo Methler
timo.methler@yahoo.de
Instituto Superior Técnico, Universidade de Lisboa, Portugal

November 2018

Abstract – The last three decades have witnessed a significant increase in the use of stepped spillways, which is closely linked to the roller compacted concrete technique applied to dam engineering. A numerical study of the flow over Pedrógão dam spillway and roller bucket using the Computational Fluid Dynamics (CFD) software code FLOW-3D® was carried out. The study embraced the analysis of CFD simulations on both prototype and physical model scales. Flow characteristics along the ogee crest, the stepped chute and the roller bucket, including flow depths and pressure heads, were evaluated and compared with those previously acquired on a physical model, assembled at the Laboratório Nacional de Engenharia Civil (LNEC). In general, a fair agreement was found between numerical and experimental flow depth and pressure head data along an initial reach of the stepped chute and the roller bucket. However, considerable differences were obtained on the pressure head on the curved reach of the ogee crest. In fact, the mesh resolution in this initial reach was found to greatly influence the pressure head. Also, non-negligible impact of CFD scaling was found with regard to the flow depth and pressure head results. In general, the model scale CFD simulations were found to provide a better agreement with the physical model data. The comparative analysis undertaken in this study indicate that CFD modelling on complex hydraulic structures, such as stepped spillways and roller buckets, remains a challenge for future research.

Keywords: stepped spillway; ogee crest; roller bucket; skimming flow; CFD simulation; FLOW-3D®;

1 Introduction

Water is one of the most basic resources necessary for life. Due to global warming or better the concentration of extreme weather occurrences, the importance of storing large amounts of water becomes more and more important. This will increase the need for water storage capabilities [1]. Relevant dam structures include necessarily a spillway, to be able to discharge excessive amounts of water. Spillways can feature a wide range of shapes. The increase in new dams and dam rehabilitation will lead to an increase in overtopping spillways. For overtopping protection roller compacted concrete (RCC) surfaces are often used, due to its comparatively cheap cost. The construction method facilitates the use of stepped spillways. Stepped spillway research has seen an increase in the last 20 years and CFD simulations are on the rise as supporting tool for the design process in new projects [2] [3] [4].

2 Stepped spillways

2.1. Preliminary remarks

The stepped spillway in general, is the concept of breaking the full-scale vertical fall into multiple smaller

sections. The resulting geometry resembles steps, where the name of this chute design is given. Typical example is given in Figure 1. Stepped spillways have a very specific set of flow behaviours [2]. This study will focus on Pedrógão stepped spillway and its terminal structure, a roller bucket basin.

Figure 1 Stepped overflow spillways: (a) Pedrógão dam [5]; (b) Melton dam in Australia [6]

2.2. Stepped spillway flow conditions

Stepped spillways develop specific and distinguished flow conditions and patterns. As main influence on the flow pattern are unit discharge, spillway slope and step height. For a given channel slope and step height, with increasing flow rate the flow regime evolves from nappe, then transition, and finally skimming flow [2] [7]. For strongly developed nappe flow the step length needs to be higher than flow depth [8]. Nappe flow is defined as series of small individual free-falling sections. The transition flow pattern occurs with larger unit discharges, where the individual steps are distinguishable, but not individual hydraulic occurrences. Skimming flow, is defined by fully submerged steps and eventually a fully aerated flow in the region downstream of the inception point [2] [9]. The steps of the chute form, on a hydrodynamic standpoint, a theoretical bottom with large macro-roughness [4]. This theoretical bottom is called pseudo-bottom and is formed from step tip to step tip [10]. Commonly a skimming flow is separated in four regions: clear water region, partially aerated flow region, fully aerated region and uniform flow region [2]. The transition between the non-aerated region and partially aerated flow regions is called inception point, where the boundary layer reaches the free surface. The prediction of this point has been subject of many studies and has been researched extensively in the past, e.g [11]. Skimming flow will be covered the present study. For the analysis undertaken, two different types of flow depth predictions will be used for comparisons, empirical and analytical flow depth predictions.

2.3. Analytical method

The flow on a stepped spillway has a developing boundary layer. The increasing thickness of the boundary layer is commonly expressed by δ, which is essential to predict the inception point. The development of δ can be obtained by [12]

$$\delta/L = 0.114 * (L/k)^{-0.311} \quad (1)$$

with, L = length along the chute and $k = h\,cos\Theta$. The velocity profile above the boundary layer region theoretically assumes free stream velocity, u_{max}, which is calculated by equation 2 (e.g., [11] [13])

$$u_{max} = \sqrt{2g(H_0 - z_0 - d\cos(\Theta))} \quad (2)$$

with u_{max}= free stream velocity, g = gravitational acceleration, H_0 upstream total head, z_0 = vertical coordinate along the channel, d = flow depth and Θ = channel slope. Based on the continuity equation

and the velocity distribution in the developing flow region, the flow depth, *d*, can be calculated from (e.g., [11])

$$q_w = u_{max} * (d - \delta/(N+1)) \quad 3$$

with $N = 3.4$ the exponent of the power law velocity distribution within the boundary layer (e.g. [12]). This is an empirical value, determined for specific hydraulic arrangements. In this case a value for steep stepped spillways was defined by Meireles et al. [12], which is close to the N=3.0 empirical value of Amador et al. [3]. Considering δ given by equation 1, the combination of equations 2 and 3 form an iteration loop, providing a flow depth prediction for a given distance along the chute. Further analyses will be based on the N value of Meireles et al. [12].

2.4. Empirical formulae

Meireles et al. [12] analysed a multitude of data sources to create an equation for empirical clear water depth predictions. Combining the prediction for length coordinate of the inception point, L_i, and the flow depth at the inception point, d_i, equations 4 and 5, are combined to equation 7 [12]

$$L_i/k = 6.75F_*^{0.76} \quad 4$$

$$d_i/k = 0.35F_*^{0.59} \quad 5$$

with, $k = h\,cos\Theta$, Θ being the chute slope. Equations 4 and 5 are shown in Figure 2 (a),(b) by Meireles et al. [12], using F^* , the roughness Froude number as,

$$F_* = q_w/\sqrt{g\sin(\Theta)\,k^3} \quad 6$$

where, q_w is the unit discharge and g the gravitational acceleration.

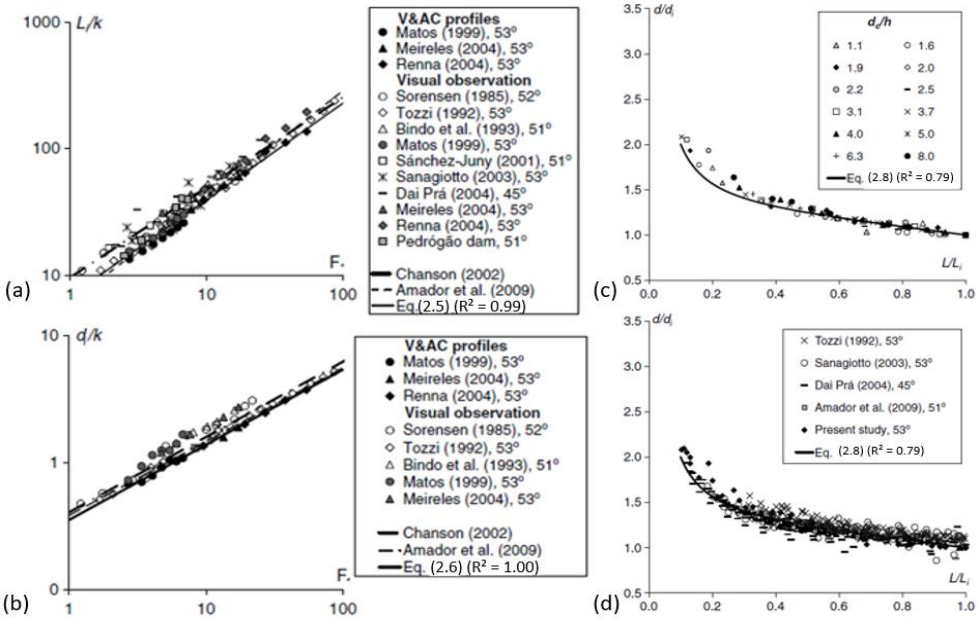

Figure 2 Flow properties in the non-aerated flow region: (a) location of the inception point; (b) equivalent clear water depth at the inception point; (c) comparison among equation 7 and experimental data from the study undertaken at LNEC (d) comparison among equation 7 and experimental data from several studies for similar slope (adapted from [12])

$$d/d_i = 1.17 - 0.25L/L_i + (0.084/(L/L_i)) \quad (7)$$

Equation 7 is only valid in the region of $0.1 \leq L/L_i \leq 1$ and for $0.4 \leq d_c/h \leq 19.3$ [12]. The critical flow depth is referred to as d_c and is calculated by $d_c = \sqrt[3]{q_w^2/g}$. Applying these equations to the case of Pedrógão dam gives $d_c/h = 9.1$ and is therefore in the applicable range for the empirical flow depth prediction method of Meireles et al. [12], provided in the correct L/L_i region. Equation 7 is plotted in Figure 2 (c),(d) by Meireles et al. [12]. The graphs show the very good agreement in the larger L/L_i regions and more deviation in the lower L/L_i region, which is significant considering that the flow on Pedrógão only reaches a L/L_i of 0.25, for the design discharge.

3 Physical model

The Pedrógão dam has been subject of model scale testing in the facilities of National Laboratory of Civil Engineering (LNEC). These studies where commissioned by EDIA (Empresa de Desenvolvimento e Infra-Estruturas do Alqueva) to reconsider the safety of the embankment protection and cavitation damage safety of the existing structure, Pedrógão dam. For this purpose, LNEC has built a 1:65 scale model of the environment of Pedrógão and the hydraulic system to sustain testing of varying unit discharges up to $12000 m^3 s^{-1}$ (scaled to prototype). The upper end of the simulation range has been determined as a 1000 year flood and determines the maximum discharge of certified safety of the structure [14]. This thesis uses the model data recorded during this safety analysis for the Pedrógão dam. The free surface elevation oscillation in the roller bucket, was documented in minimal and maximal values for the pressure head data and free surface elevation. In the LNEC testing, the river bed was modelled with gravel. Additional information informally obtained from J. Falcão de Melo, author of [14], include subjective observations that the shape changes of river bed downstream of the structure had a significant impact on the flow depth in the roller bucket. Considering the purpose of the study and small geometrical scale, the main flow measurements should be analysed with caution. As a given example, the free surface measurements were taken manually measured at the side walls. The measurements at the side walls are expected to be higher than those at the centreline, due to bulking, the magnitude of which remains to be discussed**.**

4 Numerical model implementation

4.1. Geometry and mesh

A 3-dimensional model was created in Inventor Autodesk, shown in Figure 3(a) and imported into the simulation software Flow 3D®, where the digital environment mesh was created. In the case of this study, it was chosen to orientate the mesh positioning and cell size on the dominant reoccurring step size of 0.60 m height and 0.48 m length. It was settled on three different mesh sizes, 1:3, 1:6 and 1:12, of the dominant geometrical parameter, the step height. The absolute cell size was determined by the step height divided by, 3, 6 and 12, therefore the absolute cell sizes were, 0.2, 0.1 and 0.05 m. Common practice in CFD simulation increases the cell size in the region leading up the critical region as well as in the roller bucket reach [15] [16]. A picture of all the mesh regions is shown in Figure 3(b), where the rough mesh block are the first and the last (marked in pink). More information can be found in [5].

Table 1 Mesh cell sizes and total number of cells

	Rough Mesh [m]	Fine Mesh [m]	Total Number of Cells [-]
Mesh 1:3 prototype scale	0.2	0.2	75225
Mesh 1:6 prototype scale	0.1	0.1	300900
Mesh 1:12 prototype scale	0.1	0.05	923200
Mesh 1:3 model scale	0.00308	0.00308	75225
Mesh 1:6 model scale	0.00154	0.00154	300900

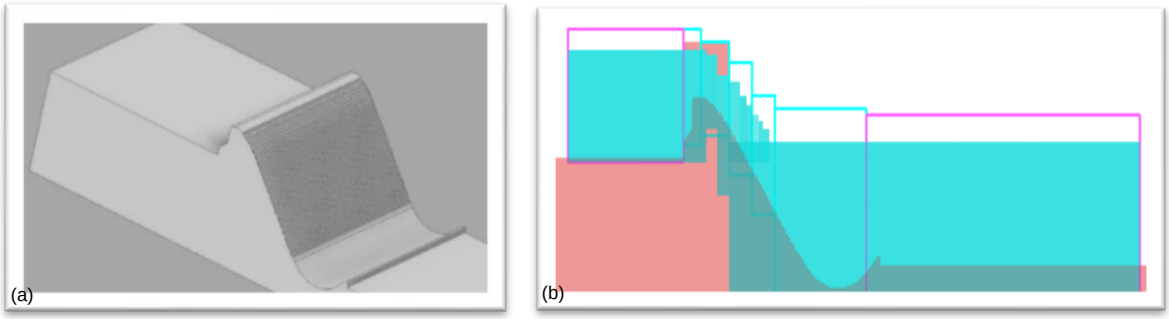

Figure 3 Geometry and mesh: (a) scheme of the 3-Dimensional model (b) mesh blocks in simulation area, rough mesh blocks marked in pink, water spawn (t=0s) regions are marked in solid light blue

4.2. Boundary conditions, steady state and physics models

Due to the common simplification in CFD simulations of assuming a 2D flow, the same was done in the executed simulations. All walls have been set with the symmetry conditions, apart from global x_{min} and x_{max}. Inflow and outflow use the static pressure condition, with a given water elevation. The water elevations were determined using the rating curves provided in [14]. In this study, the CFD simulations had to reach a steady state. Hence, an upper limit of 1% variation for 10 s was chosen for the mass-averaged turbulent kinetic energy, the mass-averaged fluid mean kinetic energy and the mass-averaged turbulent dissipation. As discussed in section 2.2, turbulence is a dominant feature of the flow over the spillway. In CFD simulation of stepped spillway hydraulics, two turbulence models are widely used, namely the $k-\epsilon$ and the RNG $k-\epsilon$, which were also adopted in the present work. More detailed information can be found in [5].

4.3. Mesh convergence

This report focuses the analyses on two different regions, the chute reach and the roller bucket reach. Therefore, two mesh flow depth convergence analyses were done independently of each other, as well as a velocity convergence analyses, all simulations compared achieved steady state. All results can be seen in [5], where averages as well as maximum deviation on single point levels are compared and evaluated.

5 Results

5.1. Flow properties

The flow depths on the chute of the stepped spillway can be compared from different methods. Figure 4 shows the empirical predictions as well as the selected CFD simulation results and the experimental results of LNEC. The flow depths were measured perpendicular to the dam surface. The minimal L/L_i border of the comparison is marked ($L/L_i = 0.097$) and represents the application range or the

analytical prediction method, together with the maximum border (L/L_i = 0.256), which indicates the beginning of the flow reach influenced by the roller bucket.

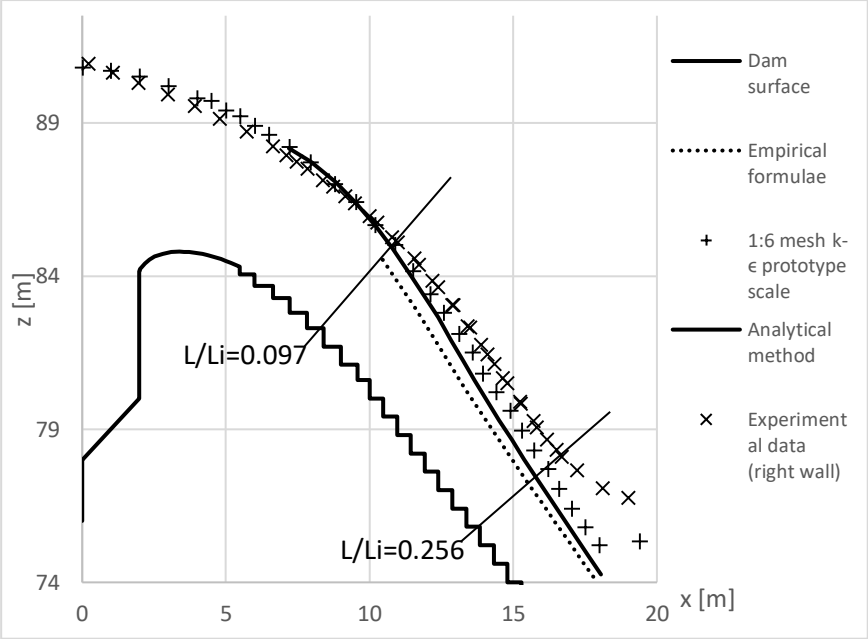

Figure 4 Free surface elevation along the chute

The flow depths are plotted in function of L/L_i along the chute, in Figure 5. The experimental flow depths are smaller in the very early parts of the chute, this reverses latest at $L/L_i = 0.08$ and the flow depths keep diverging. The empirical method, analytical method and the CFD simulations predict smaller flow depths, as seen in Figure 5. One of the main reasons for this could be the bulking at the chute walls. The experimental measurements were taken at the wall while the empirical formulae, analytical method and the CFD simulations assumed the centre of the chute cross-section.

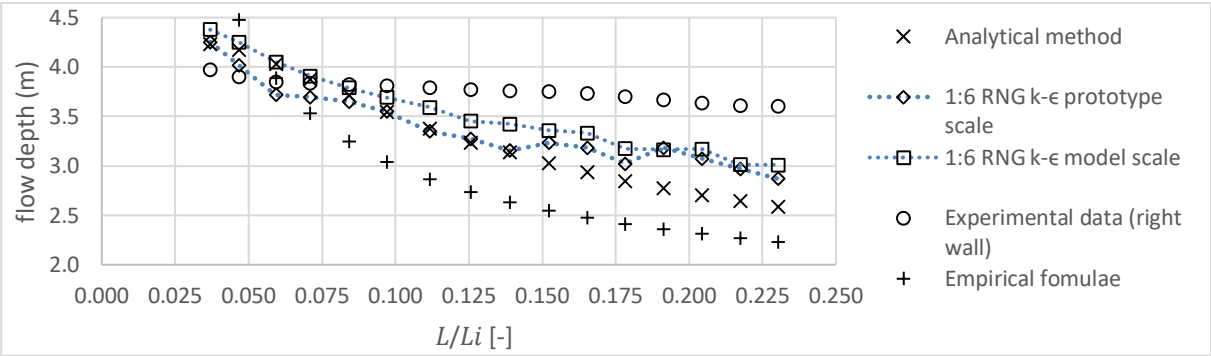

Figure 5 Flow depth along the chute

This behaviour was observed in the same way by the experiments of Bombardelli et al. [15], shown in Figure 6 (a). These experiments consisted of a very similar set up, with an ogee crest and a chute slope of 53° (Pedrógão slope = 51°). Bombardelli et al. [15] do not mention specific difference values for the shown smaller L/L_i values, visually they seem to be on average $\sim 10\%$ larger. The measurements in the experiments of Bombardelli et al. [15] were obtained in the centre of the chute cross-section and therefore do not contain bulking distortion. When comparing the prototype scale CFD simulation and the model scale CFD simulation with the experimental values, the scale simulation is closer to the

experimental values. Scaling in CFD simulations is its own research field and this comparison between the simulations clearly show that there are non-negligible effects in CFD scaling. Noteworthy in this section is the difference between the empirical formulae proposed by Meireles et al. [12] and the analytical method. Figure 2 (a),(b) showed the data the empirical formulae were derived from and its inaccuracy in the region L/L_i <0.35. For the design discharge, the flow Pedrógão spillway reaches a L/L_i = 0.25, therefore, the analytical method will be used for comparison with the CFD simulations.

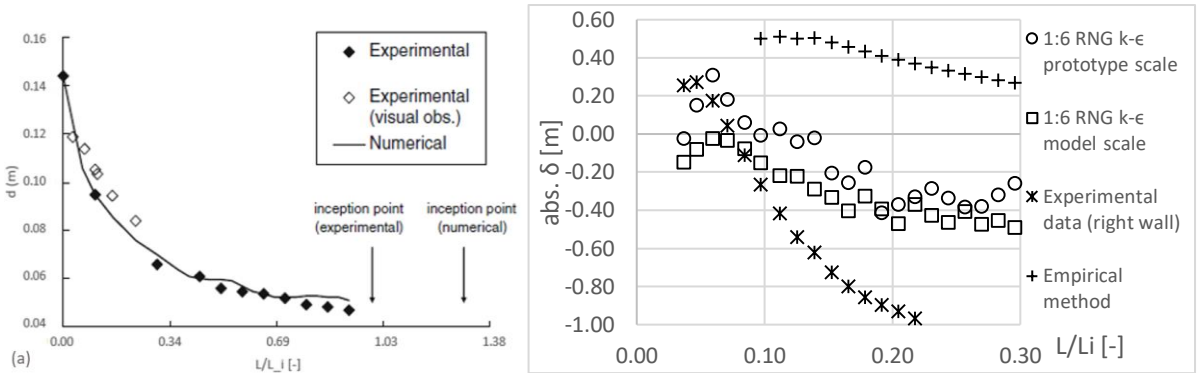

Figure 6 (a) Flow depth results by [15], adapted to have L/L_i. Axis; (b) δ absolute values, analytical method flow depths versus CFD and experimental flow depths in function of L/L_i

The comparison of the CFD results with the analytical predictions is show in Figure 6 (b), which includes the absolute differences in flow depths, of the CFD simulations and the experimental results to the analytical method predictions, along the chute, in function of L/L_i . The values in δ relative to the CFD simulation for L/L_i>0.18 show a practically constant trend. Figure 7 (a) shows the velocity profile above step 1 ($L/L_i = 0.037$) perpendicular to the pseudo-bottom. Plotted are the velocity evolution for the 1:3 and 1:6 RNG k-ϵ simulation, in function of the distance normal to the pseudo-bottom. It shows the small impact of CFD simulation mesh size, except close to the pseudo-bottom.

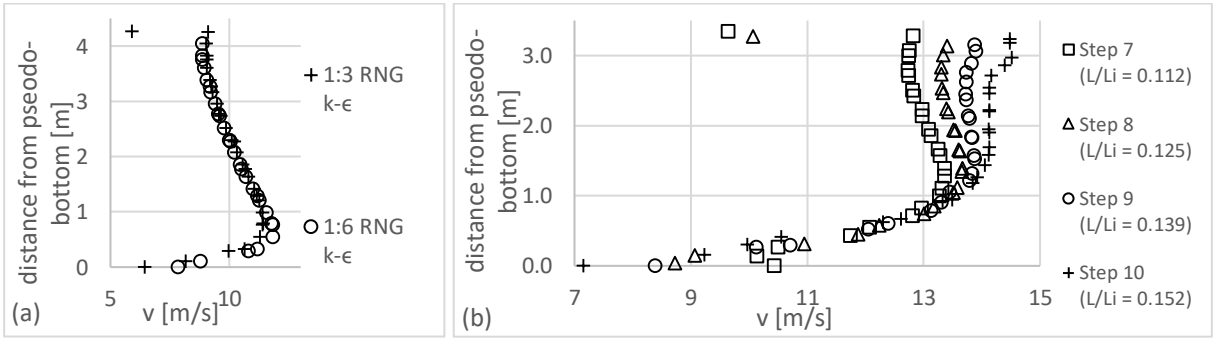

Figure 7 Velocity profiles (a) (L/L_i =0.037); (b) $L/L_i = 0.112 - 0.152$ for the 1:6 RNG $k-\epsilon$

The velocity profiles near $L/L_i = 0.2$ region evolve to the known free flow shape. This is shown in Figure 7 (b), where the velocity distributions for steps 7-10 are plotted in function of the distance to the pseudo-bottom. Step 9, where $L/L_i = 0.139$, is the first step which shows a velocity distribution typical of the flow in the chute region. Considering the convergence of δ correlating with the shift in boundary layer shape, it leads to a possible misrepresentation of the boundary layer by the CFD simulation, or the analytical method used to predict the flow depth.

The roller bucket is a turbulent flow region with an oscillating free surface. Figure 8 gives an overview

over the different free surface elevation plotted in function of the x development and with the bottom. The oscillation in flow depth is indicated at the roller bucket and at the surge location with their minimal and maximal values, for the experimental values only. Comparing the flow depths of the experimental values to the CFD simulations shows slightly lower flow depths for the simulations. Considering the indicated oscillation of the experimental values the CFD simulations are well within the range of the experimental flow depths. The general shape of the flow is easily recognizable and the average as well as the maximum relative differences in flow depths are shown in Table 2.

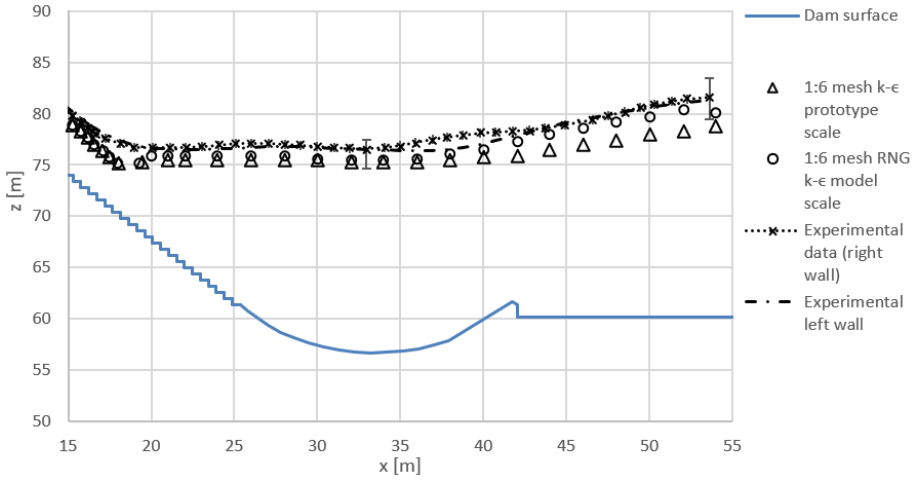

Figure 8 Free surface elevation on the roller bucket, Experimental and CFD, scale and full scale, data

Table 2 Flow depth in the roller bucket avg. δ% and max. δ%, compared with experimental results

Flow depth in the roller bucket	avg. δ%	max. δ%
Experimental to 1:6 RNG $k-\epsilon$ model scale	5.58	8.86
Experimental to 1:6 RNG $k-\epsilon$ prototype scale	10.05	14.07

The simulation at 1:65 model scale is generally closer to the experimental values, which further enforces the point of scaling effects in simulations. Figure 9 shows the δ% abs. evolution in function of the roller bucket region in comparison to the experimental flow depths. The evolution of δ% abs. in scale does not have a clear converging or diverging trend

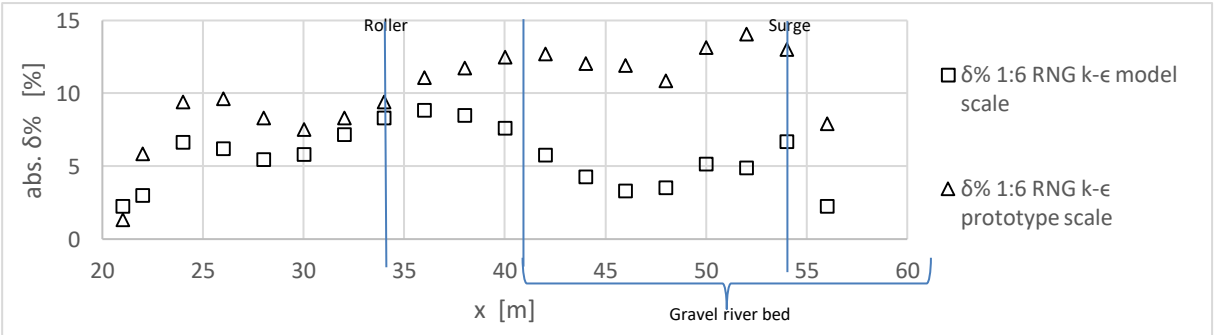

Figure 9 Flow depth relative differences along the roller bucket compared to experimental right wall

The experimental study by LNEC included a gravel river bed downstream of the roller bucket which acquired a wavy pattern due to the impact of the flow at the toe of the spillway. The pike of the pattern is located at x = 46m in the simulation environment. Flow 3D® would offer an option to simulate the scour

movement. This opens up new ways of improving CFD simulations by incorporating environmental change like this riverbed scour.

5.2. Pressure head distribution

Figure 10 shows the $\delta\%$ differences in pressure head for the different pressure taps. In the roller bucket region, the simulations stay near or in case of model simulation within 10% deviation compared to the experimental values, therefore the simulation values can be seen as good estimates.

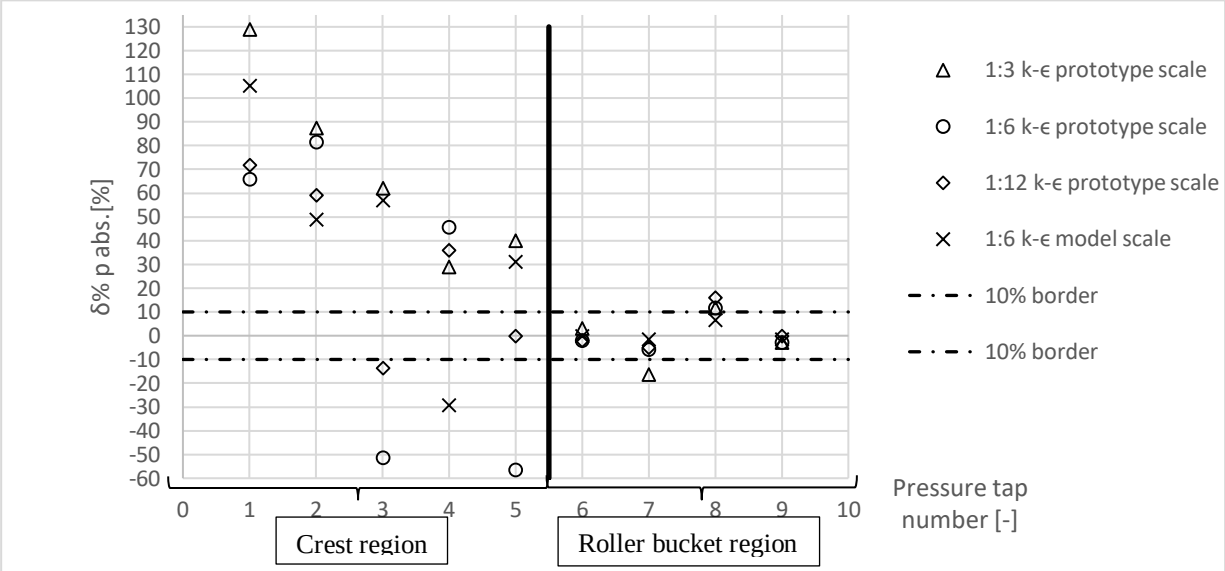

Figure 10 Pressure head differences compared to model values in %, ordered by pressure tap number

Similarly, for the crest region the $\delta\%$ shown in Figure 10 are very high compared to the experimental values. The values show a strong correlation to mesh size. This seems largely related to the averaging of pressure values over a cell. Due to this the pressures in the crest region are very sensitive to location in the CFD simulation. Figure 11 shows the pressure distribution at the crest in the 1:12 k-ϵ simulation. The visible variations need to be taken into account which is why the probes have to be positioned manually to be comparable to pressure taps. Additional information can be seen in [5].

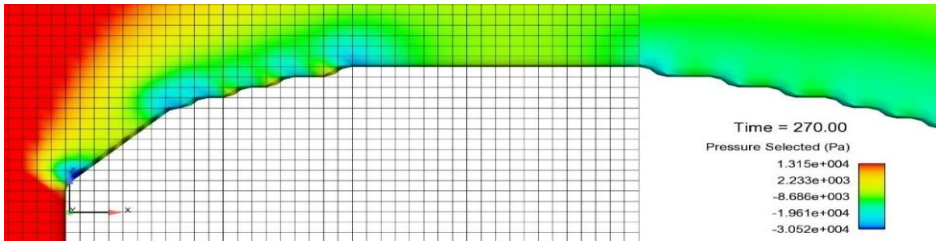

Figure 11 Pressure distribution isometric colouring view at the crest in the 1:12 $k-\epsilon$ simulation

6 Conclusion

A numerical study of the flow over Pedrógão dam spillway and roller bucket using the Computational Fluid Dynamics software code FLOW-3D® was undertaken. Significant differences were found with regard to mesh size convergence, in function of the flow region and parameters of interest. Mesh convergence was obtained for the flow depths in the roller bucket region for the 1:3 mesh, whereas in the chute region, flow depths and velocity profiles were found to converge to a satisfactory level for the

1:6 mesh size. The flow depth predictions also showed discrepancies in the developing flow region, either for the CFD simulations or for the empirical and analytical approaches. The pressure heads at the ramp of the roller bucket seemed to converge in its results in the range of the 1:6 mesh size, after manually adjusting their positions to incorporate CFD simulation related averaging errors. However, in the crest region, pressure heads did not show convergence, neither realistic values. This further suggests the misrepresentation of the flow conditions near the structure, in the vicinity of the crest. Scaling behaviour effects resulting from different simulations were shown, in all comparisons, which confirms the effort to advance in the field of CFD scaling. An ongoing dedicated study on scaling effects in CFD simulation by Torres, [17] showed average flow depth variations between 14 to 18% (low flow rates) and 4 to 6% (high flow rates) which are in the same range as the deviation shown in this thesis.

Future analyses of Pedrógão dam could yield information on scaling in CFD simulations, provided prototype flow depth data is acquired to reliably estimate bulking and get a scientifically orientated complete set of data. This data could also be used to calibrating different CFD simulations for the crest region and for the chute region in an attempt to isolate dominating parameters for the developing flow and pressure head predictions in the crest region. This might require high amounts of computational capacity due to the very small mesh size needed to reproduce adequately the flow in the crest region.

Acknowledgements: Special thanks to Prof. Jorge Matos for all the effort, Dr. José Melo for his support, EDIA the opportunity to work with a real-life project and Prof. Falcão de Campos for our study program.

References

[1] C. Zarfl, A. E. Lumsdon, J. Berlekamp, L. Tydecks and K. Tockner, "A Global Boom in Hydropower dam Construction," *Aquatic Sciences,* pp. 1-11, 8 October 2014.

[2] J. Matos and I. Meireles, "Hydraulics of Stepped Weirs and Dam Spillways: Engineering Challenges, Labyrinths of Research," in *5th International Symposium on Hydraulic Structures*, Brisbane, Australia, 2014.

[3] A. Amador, M. Sánchez-Juny and J. Dolz, "Developing Flow Region and Pressure Fluctuations on Steeply Sloping Stepped Spillways," *Journal of Hydraulic Engineering,* vol. 135, no. 12, pp. 1092-1100, 1 December 2009.

[4] R. M. Chamani and N. Rajaratnam, "Jet Flow on Stepped Spillways," *Journal of Hydraulic Engineering,* vol. 120, no. 2, pp. 254-259, 2. Febuary 1994.

[5] T. Methler, "CFD modeling of the flow over Pedrógão dam spillway and roller bucket," MSc Thesis, Lisbon, 2018

[6] H. Chanson, "Melton Dam Overflow Stepped Spillway, Australia," 2000. [Online]. Available: http://staff.civil.uq.edu.au/h.chanson/pictures/melton2a.jpg.

[7] H. Chanson, "Prediction of the Transition Nappe/Skimming Flow on a Stepped Channel," *Journal of Hydraulic Research,* vol. 34, no. 3, pp. 421-429, 1996.

[8] M. Lejeune and A. Lejeune, "About the Energy Dissipation of Skimming Flows Over Stepped Spillways," in *1st International conference, Hydroinformatics*, Delft, Netherlands, 1994.

[9] M. Bindo, J. Gautier and F. Lacroix, "The Stepped Spillway of M'Bali Dam," *International Water Power and Dam Construction,* vol. 45, pp. 35-36, January 1993.

[10] A. C. Gonzalez and H. Chanson, "Interactions Between Cavity Flow and Main Stream Skimming Flows," *Canadian Journal of Civil Engineering,* vol. 31, no. 1, pp. 33-44, 2004.

[11] H. Chanson, "Hydraulics of Stepped Chutes and Spillways," Balkema, Lisse, Netherlands, 2002.

[12] I. Meireles, F. Renna, J. Matos, F. Bombardelli and A. M. ASCE, "Skimming, Nonaerated Flow on Stepped Spillways over Roller Compacted Concrete Dams," *Journal of Hydraulic Engineering,* vol. 138, no. 10, pp. 870-877, October 2012.

[13] H. Ramos, A. Betâmio de Almeida, M. M. Portela and H. Pires de Almeida , "Guidelines for Design of Small Hydropower Plants", 1st ed., Belfast, North Ireland: Western Regional Energy Agency & Network, 2000.

[14] J. Melo, "Barragem de Pedrógão. Estudo em Modelo Reduzido do Descarregador de Cheias e da Descarga Auxiliar," NRE, LNEC, Lisbon, 2003.

[15] F. A. Bombardelli, I. Meireles and J. Matos, "Laboratory Measurements and Multi-Block Numerical Simulations of the Mean Flow and Turbulence in the Non-Aerated Skimming Flow Region of Steep Stepped Spillways," *Environ Fluid Mech,* pp. 263-288, 2011.

[16] Flow Science Inc., "Flow3D User Manual," 2012.

[17] C. Torres, D. Borman, A. Sleigh and D. Neeve, "Determination of Scale Effects for a Scaled Physical Model of a Labyrinth Weir Using CFD," in *7th International Symposium on Hydraulic Structures*, Aachen, Germany, 2018.